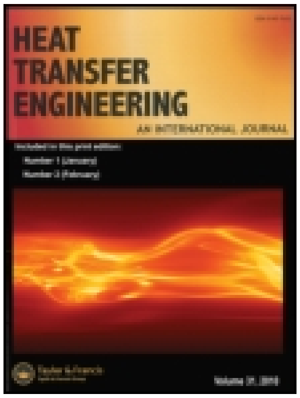

Heat Transfer Engineering
Publication details, including instructions for authors and subscription information:
http://www.tandfonline.com/loi/uhte20

Influence of Inlet Configurations on the Refrigerant Distribution of a Dual Cold-Plate System

Kai-Shing Yang [a], Kun-Huang Yu [b], Ing-Youn Chen [b] & Chi-Chuan Wang [c]

[a] Department of Electro-Optical and Energy Engineering, Ming Dao University, Changhua, Taiwan

[b] Mechanical Engineering Department, National Yunlin University of Science and Technology, Yunlin, Taiwan

[c] Department of Engineering, National Chiao Tung University, Hsinchu, Taiwan

Published online: 12 Oct 2011.

To cite this article: Kai-Shing Yang, Kun-Huang Yu, Ing-Youn Chen & Chi-Chuan Wang (2010) Influence of Inlet Configurations on the Refrigerant Distribution of a Dual Cold-Plate System, Heat Transfer Engineering, 31:8, 692-698, DOI: 10.1080/01457630903466688

To link to this article: http://dx.doi.org/10.1080/01457630903466688

Heat Transfer Engineering, 31(8):692–698, 2010

ISSN: 0145-7632 print / 1521-0537 online
DOI: 10.1080/01457630903466688

Influence of Inlet Configurations on the Refrigerant Distribution of a Dual Cold-Plate System

KAI-SHING YANG,[1] KUN-HUANG YU,[2] ING-YOUN CHEN,[2] and CHI-CHUAN WANG[3]

[1]Department of Electro-Optical and Energy Engineering, Ming Dao University, Changhua, Taiwan
[2]Mechanical Engineering Department, National Yunlin University of Science and Technology, Yunlin, Taiwan
[3]Department of Engineering, National Chiao Tung University, Hsinchu, Taiwan

This study examines the refrigerant distribution of a dual cold-plate system subject to the influence of heating load and inlet configurations. Three inlet configurations, namely, uniformly divided, side-entrance, and inlet inclination, are examined. For an unequal heating load for both uniformly divided and side-entrance configurations, it is found that the distribution of mass flow rate subject to the influence of heating load is strongly related to the outlet states of the two cold plates. For the condition where one of the cold plates is in a superheated state while the other is in a saturated state, the mass flow rate pertaining to a fixed heating load is lower than that of a smaller heating load, and the difference increases significantly when the heating load gets smaller. For the condition where both outlet states of cold plate are at superheated states, the mass flow rate for the fixed heating load is about the same for the uniformly divided configuration and is marginally higher than that of the smaller heating load at the side-entrance configuration. The inlet inclination has a moderate influence on the flow distribution; the difference in mass flow rate is as large as 15% when the inclination angle is 10°.

INTRODUCTION

During the past several decades, the performance of semiconductor device doubled (Moore [1]) every 18 months, primarily due to the improvement of lithography-based microfabrication. However, the improvement of lithography-based microfabrication may soon approach its physical limit of light and materials. Although seeking and developing new material to lengthen the limit of the Moore's law is a quite challenging research issue, there are also some alternative methods to augment the performance of semiconductor devices without adopting new materials. For instance, semiconductor devices operating at a low temperature can be drastically improved (Taut et al. [2]). This is because of faster switching time of semiconductor devices and increased circuit speed due to lower electrical resistance of interconnecting materials at low temperatures (Balestra and Ghibaudo [3]). Depending on the doping characteristics of the chip, attainable performance improvements range from 1% to 3% for every 10°C lower transistor temperature (Phelan [4]). In addition to the physical limit of shrinking the size of integrated circuit, there also arises a considerable heat dissipation that must be managed. As a consequence, advanced electronic products all suffers from the rapid rise of cooling demand. The conventional air cooling featuring low heat transfer performance and noise problems is no longer able to handle high-flux applications, yet alternatives like heat pipes, liquid immersion, jet impingement and sprays, thermoelectrics, and refrigeration (Trutassanawin et al. [5]) are considered to be powerful solutions. Of the forgoing alternatives, refrigeration is not only reliable but also can operate at a sub-ambient condition that is quite demanding for high-heat-flux applications.

Some investigations were reported for cooling of electronic devices via refrigeration. These studies are related to the fundamental system performance such as junction to ambient air thermal resistance, system coefficient of performance (COP) of the refrigeration system (Phelan and Swanson [6]), and transient response behavior (Nnann [7]). Some refrigeration cooling systems for electronics are already commercially available,

The authors are indebted to the financial support of the Bureau of Energy and Department of Industrial Technology, the Ministry of Economic Affairs, Taiwan.

Address correspondence to Dr. Chi-Chuan Wang, EE474, 1001 TA Hsueh Road, Hsinchu, Taiwan 30010, Republic of China. E-mail: ccwang@itri.org.tw

e.g., the IBM S/390 G4 CMOS server system (Schmidt and Notohardjono [8]) and KryoTech super G computer (Peeples [9]). In this study, efforts are made toward simulation of the high-end application having dual chip devices. As is known for the high-end computational applications, the system may require multiple chips for parallel processing. Depending on the demand, the chip may operate in full or partial load, thereby resulting in varying heat dissipation of each chip. However, this may lead to certain problems for the refrigeration system because variable heat load gives rise to variation in fluid volume. In this sense, refrigerant distribution into cooling chips may vary as it is being evaporated. As a result, the objective of this study to explore the associated refrigerant distribution characteristics subject to operation conditions of refrigeration systems.

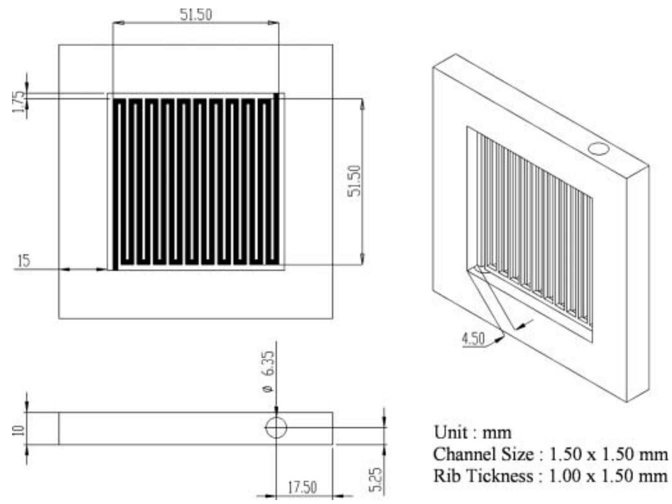

Figure 2 Detailed dimension of the cold-plate heat sink.

EXPERIMENTAL SETUP

A schematic of the whole experimental system is shown in Figure 1. The system is basically a refrigeration system, including a variable-speed drive compressor, a double-pipe condenser, a metering valve and a capillary tube as the expansion device, and two identical serpentine cold plates as the evaporators. The mini-rotary compressor is provided by TECO Corporation with an outer cylinder diameter of 60 mm and a length of 100 mm, having a total weight of 1.2 kg. The mini compressor is an R-134a-based DC-driven compressor with an adjustable cooling capacity ranging from 50 to 250 W. The condenser is a water-cooled double-pipe condenser.

During the operation, water is circulated at the annulus of the double-pipe condenser, whereas refrigerant is flowing inside the tube. A manually controlled metering expansion valve (HOKE 1300 series) is located at the exit of condenser. For easier manipulating and stabilizing of the system performance, an extra capillary tube with an inner diameter (ID) of 1 mm and a length of 300 mm is placed right after the metering valve. When the refrigerant leaves the capillary tube, it then splits by a T-junction into two identical cold plates. The cold plate is of square configuration, with effective internal volume of 51 × 51 × 4.5 mm (H). Detailed dimensions of the cold plate are shown in Figure 2. As seen in the figure, two-phase refrigerant enters into the cold plate at the corner of the side plate; it then evaporates along the serpentine channel. A Kapton heater with a size almost identical to the base effective size (50.8 × 50.8 mm) adheres below the cold plate to simulate the heat source and to eliminate the spreading resistance. An insulation box made of Bakelite with a low thermal conductivity of 0.233 W/m^{-}K is placed beneath the heater to reduce the heat loss. In addition, a high-thermal-conductivity grease ($k = 2.1$ W/m^{-}K) is used to connect the heat sink and the heater. For further minimization of the contact resistance, four M4 screws with fixed applied pressure located at the corners of the base plate are employed. The heater is regulated with a DC power supply.

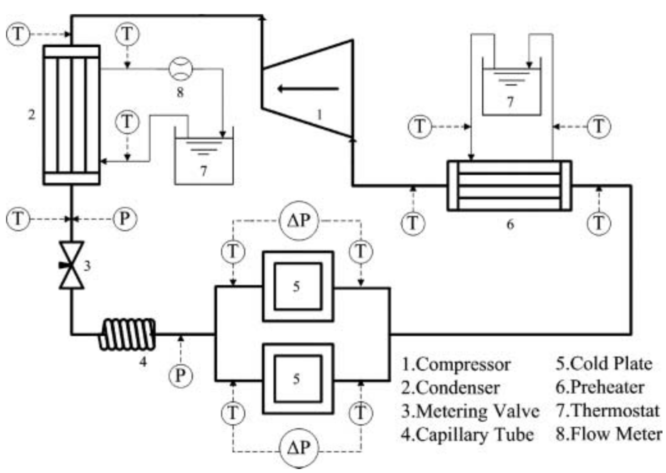

Figure 1 Schematic of the test apparatus.

For recording the performance of the refrigeration system, two precise pressure transducers (YOKOKAWA, EJA530A with an accuracy of ±0.2%) are used to measure the condensing and evaporation pressure of the refrigerant system, respectively. A magnetic flowmeter (YOKOKAWA, ADMAGAE110MG) with a calibrated accuracy of 0.1% is employed to the measurements of water mass flow rate in the cooling loop to the condenser. Resistance temperature devices with a calibrated accuracy of 0.1°C are installed at the refrigerant circuitry, whereas 5 T-type thermocouples are used for measurements of the wall surfaces of the cold plate. The differential pressure transducers are from YOKOKAWA EJA110A, which is accurate to 0.1% of the measuring span.

During the experiment, suitable adjustments of the system are made to ensure the inlet and outlet states of the condenser to be in superheated and subcooled conditions. In the meantime, the heat capacity of the condenser can be obtained via the energy balance of the cooling water:

$$\dot{Q}_{cond} = \dot{m}_{water} c_p (T_{water,out} - T_{water,in}) \tag{1}$$

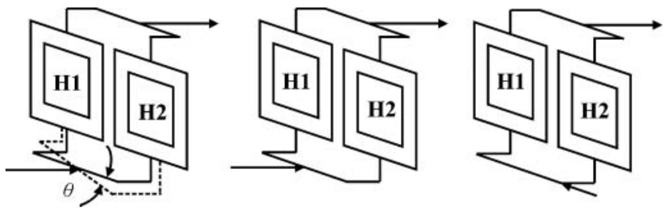

Figure 3 Schematic diagram of inlet inclinations: (a) inlet inclination; (b) uniformly divided; and (c) side entrance.

Apart from this condenser capacity, one can easily identify the enthalpy change of the refrigerant across the condenser, leading to an estimation of the total refrigerant mass flow rate by the following relationship:

$$\dot{m}_{134a,total} = \frac{\dot{Q}_{cond}}{\Delta i_{cond}} \tag{2}$$

where Δi_{cond} represents the enthalpy difference of the refrigerant flow across condenser based on the states of measured inlet superheating and outlet subcooling temperatures. The mass flow rate of the cold plates, designated as H1 and H2, can be obtained using similar estimation of the refrigerant flow at the condenser, i.e.,

$$\dot{m}_{134a,\mathrm{H1}} = \begin{cases} \frac{\dot{Q}_{H1}}{\Delta i_{H1}} \text{ (if outlet of H1 is at superheated state)} \\ \dot{m}_{total} - \dot{m}_{134a,\mathrm{H2}} \text{ (if outlet of H1 is saturated)} \end{cases}$$
$$\dot{m}_{134a,\mathrm{H2}} = \begin{cases} \frac{\dot{Q}_{H2}}{\Delta i_{H2}} \text{ (if outlet of H2 is at superheted state)} \\ \dot{m}_{total} - \dot{m}_{134a,\mathrm{H1}} \text{ (if outlet of H2 is saturated)} \end{cases} \tag{3}$$

In this study, there are three configurations in association with the influence of inlet conditions being examined. The inlet geometric conditions are as classified as uniformly divided (UD), side-entrance (SE), and inlet inclination (II), as shown Figure 3. The overall uncertainty of the reduced mass flow rate is less than 3.6% throughout the test range.

RESULTS AND DISCUSSION

For a uniformly divided inlet, the effect of variable heat load on the flow distribution is shown in Figure 4. In Figure 4a, the heating load of the cold plate is initially 50 W for both cold plates and the heating load to cold plate H1 is gradually increased to 70 W. Conversely, in Figure 4b tests are conducted at a fixed heat load (50W) initially, and then heating load to one of the cold plate (H1) remains fixed whereas the heat load to the other cold plate (H2) is gradually reduced from 50 W to 30 W.

As expected, at the beginning of the experiment heat loading to each cold plate is identical (50 W), and thus refrigerant distribution to each cold plate is almost the same. For the gradually increased of heating load to H1, as shown in Figure 4a, it seems that there is no considerable difference of mass flow rate between these two cold plates. This is because the outlets for both cold plates are in a superheated state (Figure 5a); hence additional contribution of pressure drop caused by acceleration

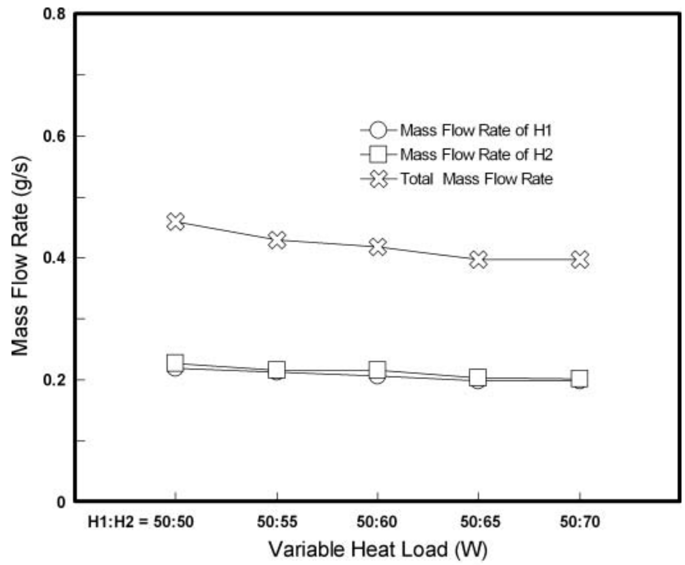

(a)

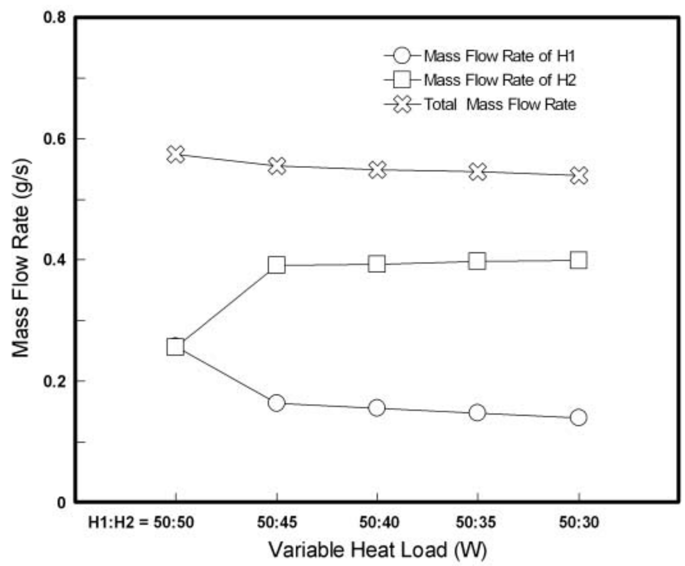

(b)

Figure 4 Influence of (a) increasing or (b) reducing heating load of H2 on the mass flow rate distribution of cold plate H1 and H2 in diverge configurations.

(ΔP_a) is rather small, suggesting the major influence of changing heating load on the refrigerant flow distribution comes from the percentage distribution between the two-phase region and single-phase region. It is expected that a larger heating load for H1 gives rise to a smaller two-phase portion while retaining more for the single-phase region, as appeared. For a normal evaporation process, the pressure gradient ($\Delta P/\Delta z$) rises with vapor quality; it may reach a maximum around a vapor quality of 0.6–0.8 and then decline thereafter to the single-phase condition when superheated. Normally the pressure gradient for two-phase flow at a low-quality region is lower than that of the vapor phase but is much larger at a high-quality region. In this sense the refrigerant flow into H1 must adjust itself to be slightly

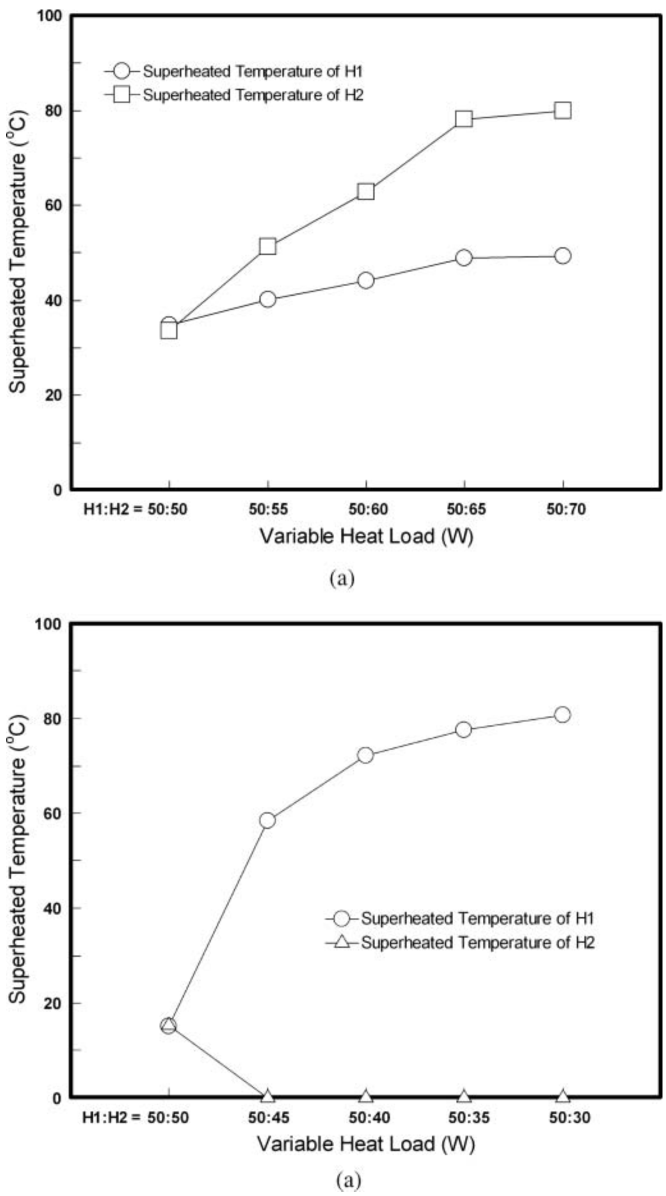

Figure 5 Influence of (a) increasing or (b) reducing heating load of H2 on the superheated temperature of cold plate H1 and H2 in diverge configurations.

higher in order to maintain the fixed ΔP constraint. In the meantime, there is a counterbalance from the effect of superheated temperature. A rise of heating load for H1 inevitably increases the outlet superheated temperature for H1. This will lead to a lager effective Reynolds number for the single-phase region, and a larger pressure drop accordingly. As a result, the contribution of the single-phase pressure drop offsets the contribution of two-phase friction, resulting in a nearly unchanged difference of refrigerant flow for H1 and H2 with a further increase of heating load.

However, there is a considerable departure of flow-rate distribution for reducing heating load of H2, as shown in Figure 4b; one can see that an uneven refrigerant flow distribution occurs. The flow rate in H2 with a lower heat loading is conspicuously higher than that in H1. The uneven refrigerant flow distribution subject to change of heating load is related to variation of flow resistance and the outlet status of refrigerant flow within each cold plate. The major effect of changing heat load on the overall pressure drop is from ΔP_a arising from vaporization. A rough estimate of the contribution of this term can be found from Collier and Thome [10]:

$$\Delta P_a \approx \int_{x_{in}}^{x_{out}} G^2 \left(\frac{1}{\rho_G} - \frac{1}{\rho_L}\right) dx$$

$$\approx G^2 \left(\frac{1}{\rho_G} - \frac{1}{\rho_L}\right)(x_{out} - x_{in}) \tag{4}$$

With a drop of heating load, the contribution of this term is further reduced. The influence of this term is especially amplified when the outlets of both cold plates are different, i.e., one at the superheated sate and the other at the saturated condition (Figure 5b). When the supplied heat at H2 is reduced to a condition such that the outlet state of H2 is saturated, the contribution of ΔP_a is dramatically reduced. However, the measured total pressure drop ΔP remains the same for cold plate H1 and H2 ($\Delta P_{H1} = \Delta P_{H2}$) since the refrigerant flow is under splitting and recombining. If the mass flow rate of H1 and H2 is still the same, it will result in a larger ΔP_{H1}. To meet the constraint of $\Delta P_{H1} = \Delta P_{H2}$, the refrigerant flow into H2 must exceed H1. As shown in Figure 6, the flow rates of both cold plates are equal initially (point 1). When the outlet condition of H2 changes from superheated region to saturated stage (point 2), it will introduce a considerable amount of mass flow rate subject to significant reduction of acceleration pressure drop and frictional pressure drop. Although the increased mass flow rate may result in a larger pressure drop, it should be emphasized that the effect is counterbalanced by the resulting low pressure gradient of two-phase flow at the low-quality region. Therefore, the pressure drop may be substantially decreased, leading to a considerable rise of mass flow rate at the two-phase region. An analysis and experimental results presented by Minzer et al. [11] for the water flowing in evaporating pipes confirmed the

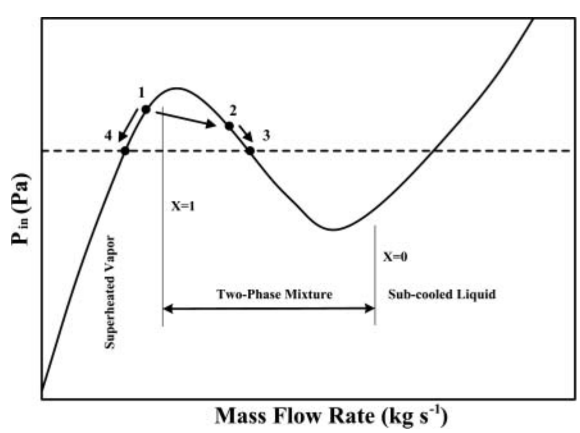

Figure 6 Pressure difference along a single pipe versus flow rate subject to two-phase flow condition.

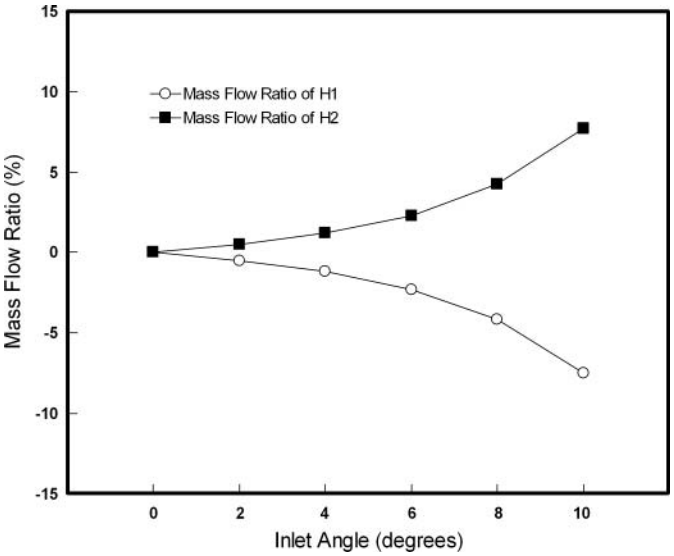

Figure 7 Influence of inlet angle of H1 on the mass flow rate distribution of cold plate H1 and H2.

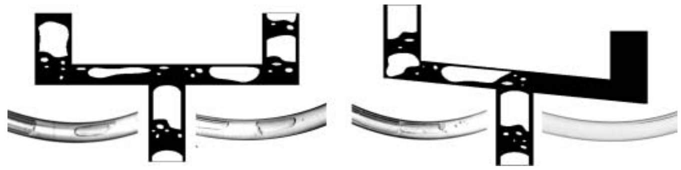

Figure 8 Schematic presentation of the asymmetric case on inlet angle.

present result. The lower ΔP_{H2} must also meet the constraint of $\Delta P_{H1} = \Delta P_{H2}$, and the refrigerant flow into H2 must exceed H1 again. As a result, one can see that the mass flow rate ratio of H2 is continuously increased and the pressure drop is continuously decreased with a further reducing heat load at H2. In the meantime, the condition of H1 is still at the superheated state; the decline of flow rate of H1 causes the pressure drop to become even smaller. Eventually the pressure drops of H1 and H2 will balance at point 4 and point 3, respectively, as shown in Figure 6, but with a tremendous difference in magnitude as compared to Figure 4b.

Figure 7 shows the influence of inlet inclination on the distribution of mass flow rate for the cold plates H1 and H2. The inlet quality is 0.01, yet the inlet piping of H2 is below the piping of H1, as shown in Figure 3a. With this arrangement, the refrigerant flow into H2 is expected to exceed H1 when increasing the inlet inclination angle due to the influence buoyancy. The difference of mass flow ratio is increased to 15% when the inclination angle is raised to 10°. The flow pattern at the inlet section is elongated bubble flow due to its low inlet quality. In Figure 8, one can see a schematic showing the asymmetric flow into the two cold plates. Tshuva et al. [12] also observed that the asymmetric flow becomes more and more pronounced when the inclination angle is increased, yet this phenomenon is especially evident at a low flow rates. The asymmetric flow results in a higher inlet quality of H1, and correspondingly a higher pressure drop. As a consequence, the flow rate for H1 must dwindle to some extent to meet the constraint of $\Delta P_{H1} = \Delta P_{H2.}$

Figure 9 shows the total mass flow rate and individual mass flow rate ratio for each cold plate subject to change of heat load for a side-entrance condition. For easier understanding about the difference between uniformly divided and side-entrance inlet, the first data point of Figure 9 is the initial reference state for a uniformly divided inlet at a heat load of 50 W. Following the first data point on the right is the result of an initial state of side-entrance. As seen, the mass flow rate of H1 exceeds that of H2 by approximately 20%. In the first place, this is somehow expected, for the least portion of the entering flow is forced to turn around into H2. However, there is an additional two-phase redistribution effect occurring at the inlet that reinforces the flow distribution. This phenomenon can be made clear from a typical flow distribution of a bottom-dividing header of a heat exchanger conducted by Webb and Chung [13]. They found that the two-phase flow will be vapor-rich near the pass inlet, whereas it is liquid-rich near the end of the pass. Therefore, the pressure gradient of H1 is lower than for H2 pertaining to its lower quality (liquid-rich). Hence the higher pressure drop of H2 leads to more refrigerant flow into H1. The higher mass flow into H1 reduces the average quality since these two cold plates are initially at the same heating load, and thereby the pressure drop becomes smaller.

With a further reduction of heat load from 50 W to 45 W for H1, one can see that the outlet condition for H2 turns into a saturated region. The effect is similar to the foregoing results for reducing heating load of H2 for a uniformly divided situation as shown in Figure 4b. The significant rise of mass flow rate of H1 is seen with a further reducing heat load. However, there is only a slightly variation of flow rate distribution for reducing heating load of H2 with the side-entrance condition as shown in Figure 10. Again, initially the inlet of H2 reveals a lower mass flow rate than H1 with a higher quality (vapor-rich). However,

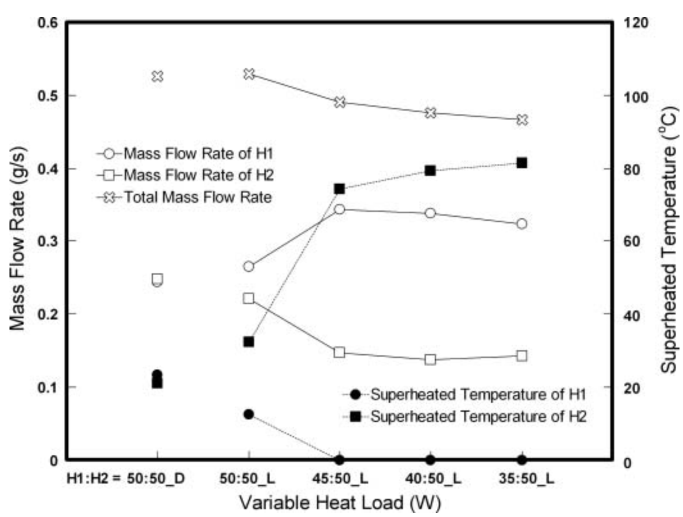

Figure 9 Influence of increasing heating load of H1 on the (a) mass flow rate distribution and (b) superheated temperature of cold plate H1 and H2 at side entrance configuration.

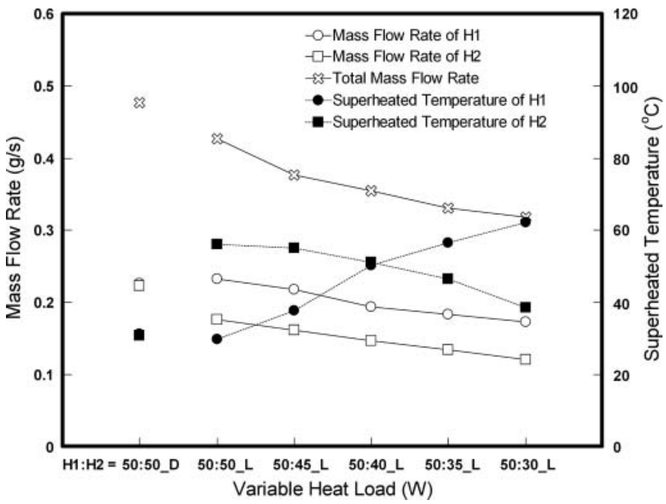

Figure 10 Influence of reducing heating load of H2 on the (a) mass flow rate distribution and (b) superheat temperature of cold plate H1 and H2 at side entrance configuration.

since the outlet condition for both cold plates maintains as superheated even when the heat load is reducing from 50 W to 30 W as shown in Figure 10, in this case, the situation for tremendous change of flow rate as illustrated in Figure 6 will not happen. The major effect of refrigerant flow distribution subject to change of heating load is related to variation of flow resistance and the outlet status of refrigerant flow within each cold plate. There is no significant mass flow rate variation when the outlet statuses of refrigerant flow both in cold plates are superheated.

CONCLUSIONS

This work has been an experimental study conducted to examine the refrigerant distribution of a dual cold-plate system subject to the influence of heating load and inlet configurations using R-134a as the working fluid. Three different inlet flow configurations are examined in this study, including uniformly divided, side-entrance, and inlet inclination. For a uniformly divided inlet, it is found that the unequal heating load imposes a decisive influence on the flow rate distribution. In general, there is negligible effect of heat load on the distribution of mass flow rate provided that the outlets of both cold plates are at superheated region. Conversely, a dramatic change of mass flow rate is seen when one of the outlet of one cold plate is saturated whereas the other is superheated.

The effect of inlet inclination has a moderate influence on the mass flow distribution. The maldistribution normally becomes more and more pronounced with the rise of inclination angle, and the difference can be as large as 15% for an inclination angle of 10°.

For the effect of the side-entrance inlet, unequal refrigerant distribution prevails even with the same heating load. This is related to vapor-rich flow near the pass inlet while liquid-rich flow occurs the downstream. In the meantime, the flow distribution is similar to that of uniformly divided conditions. A significant difference in mass flow rate is seen if the outlet states of the cold plates are not the same, whereas the difference is rather small when both outlets are superheated.

NOMENCLATURE

c_p	specific heat (J/kg-K)
G	mass flux (kg/m^2-s)
i	enthalpy (J/kg)
k	thermal conductivity (W/m-K)
$\dot{m}$	mass flow rate (kg/s)
P	pressure (Pa)
$\dot{Q}$	heat transfer rate (W)
q	heat flux (W/m^2)
T	temperature (K)
x	vapor quality

Greek Symbols

ρ	density (kg/m^3)
Δi	enthalpy difference (J/kg)
ΔP	pressure drop (Pa)

Subscripts

cond	condenser
G	vapor phase
H1	cold plate 1
H2	cold plate 2
in	inlet
L	liquid phase
out	outlet
134a	R-134a refrigerant side
total	total mass flow rate
water	water side

REFERENCES

[1] Moore, G. E., Progress in Digital Integrated Electronics, *IEEE International Electron Devices Meeting (IEDM) Digest of Technical Papers*, Washington, DC, pp. 11–13, 1975.

[2] Taut, Y., Buchanan D. A., Chen, W., Frank, D. J., Ismail, K. E., Lo, S., Sai-Halasz, G. A., Viswanathan, R. G., Warm, H. C., Wind, S. J., and Wong, H., CMOS Scaling into the Nanometer Regime, *Proc. IEEE,* vol. 85, no. 4, pp. 486–504, 1997.

[3] Balestra, F., and Ghibaudo, G., Brief Review of the MOS Device Physics for Low Temperature Electronics, *Solid-state electronics*, vol. 37, pp. 1967–1975, 1994.

[4] Phelan, P. E., Current and Future Miniature Refrigeration Cooling Technologies for High Power Microelectronics, *in Proc.*

Semiconductor Thermal Measurement and Management Symp., San Jose, CA, pp. 158–167, 2001.

[5] Trutassanawin, S., Groll, E. A., Garimella, S. V., and Cremaschi, L., Experimental Investigation of a Miniature-Scale Refrigeration System for Electronics Cooling, *IEEE Trans. On Component and Packaging Technologies*, vol. 29, pp. 678–687, 2006.

[6] Phelan, P. E., and Swanson, J., Designing a Mesoscale Vapor-Compression Refrigerator for Cooling High-Power Microelectronics, in *Proc. Intersociety Conference on Thermal and Themomechical Phenomena in Electronic Systems (I-THERM)*, Las Vegas, NV, pp. 218–223, 2004.

[7] Nnann, A. G. A., Application of Refrigeration System in Electronics Cooling, *Applied Thermal Engineering,* vol. 26, pp. 18–27, 2006.

[8] Schmidt, R. R., and Notohardjono, B. D., High-End Server Low-Temperature Cooling, *IBM Journal of Research and Development,* vol. 46, pp. 739–751, 2002.

[9] Peeples, J. W., Vapor Compression Cooling for High Performance Applications, *Electronics Cooling,* vol. 7, pp. 16–24, 2001.

[10] Collier, J. G., and Thome, J. R., *Convective Boiling and Condensation*, 3rd ed., Oxford University Press, Oxford, 1994.

[11] Minzer, U., Barnea, D., and Taitel, Y., Evaporation in Parallel Pipes—Splitting Characteristics, *International Journal of Multiphase Flow*, vol. 29, pp. 1669–1683, 2003.

[12] Tshuva, M., Barnea, D., and Taitel, Y., Two-Phase Flow in Inclined Parallel Pipes, *International Journal of Multiphase Flow*, vol. 25, pp. 1491–1503, 1999.

[13] Webb, R. L., and Chung, K., Two-Phase Flow Distribution to Tubes of Parallel Flow Air-Cooled Heat Exchangers, *Heat Transfer Engineering*, vol. 26, pp. 3–18, 2005.

Kai-Shing Yang is currently an assistant professor in the Department of Electro-Optical and Energy Engineering, Ming Dao University Changhua, Taiwan. He received his M.S. and Ph.D. degrees in mechanical engineering from the National Yunlin University of Science and Technology, Taiwan during 1998–2004. He joined Ming Dao University in 2009. His research areas include enhanced heat transfer and multiphase system technology.

Kun-Huang Yu is currently a master's level student at National Yunlin University of Science and Technology, Taiwan. He received his B.S. degree from the Department of Mechanical and Automation Engineering, Da-Yeh University in 2006. His research area is multiphase system technology.

Ing-Youn Chen is currently a professor of mechanical engineering at the National Yunlin University of Science and Technology, Taiwan. He received his B.S. in mechanical engineering from National Taiwan University in 1971, and his M.S. in 1979 and Ph.D. in 1984 in mechanical engineering from Wisconsin University–Milwaukee, Milwaukee, WI. He joined Sundstrand and McDonnell Douglas space companies from 1985 to 1989 and from 1989 to 1994, respectively. In these periods, he was involved in the analysis and testing of two-phase thermal control systems for the international space station. Currently, he teaches and conducts research in two-phase flow and heat transfer areas. He is also a reviewer for several international journals.

Chi-Chuan Wang is currently a professor at National Chiao Tung University, Hsinchu, Taiwan. He received his B.S., M.S., and Ph.D. degrees all in mechanical engineering from National Chiao-Tung University, during 1978–1989. He joined Industrial Technology Research Institute in 1989 and stayed there until 2010. His research areas include enhanced heat transfer, multiphase system, micro-scale heat transfer, and heat pump technology. He is also a regional editor of the *Journal of Enhanced Heat Transfer* and an associate editor of *Heat Transfer Engineering*.